# Photo-Impedance of the AgCl Electrode System*†

D. A. WIEGAND
*Engineering Physics Department, Cornell University, Ithaca, New York and Physics Department, Carnegie Institute of Technology, Pittsburgh, Pennsylvania*

(Received May 10, 1961)

The observed frequency response of the AgCl-electrode system indicates an equivalent parallel combination of capacitance and conductance in series with the bulk photoconductance. The voltage dependence of the capacitance suggests an exhaustion layer, presumably at the sample-electrode interface, and the magnitude of the capacitance indicates that the layer is thick. Qualitatively, the dependence of the layer capacitance and current on the intensity and wavelength of the exciting illumination, on temperature, and on voltage can then be understood in terms of a potential barrier. Alternatively, the results can be described in terms of layers, presumably at the surface, of lower conductivity than the bulk. An increase of the capacitance with the bulk conductivity, and so with the density of mobile electrons, suggests that the positive charge in the exhaustion region is determined at least in part by holes generated by illumination. The dependence of the bulk photoconductivity on temperature, voltage, intensity, and wavelength are discussed.

## I. INTRODUCTION

PHOTOCONDUCTIVITY experiments permit the study of such quantities as electron and hole densities, lifetimes, mobilities, and trapping characteristics. However, in interpreting the results of a photoconduction experiment, it is almost always necessary to make assumptions concerning the effects of space charges and barriers, internal or at the electrodes, on the quantities of interest. It is often possible, however, to deduce these effects by measuring the impedance of the photoconductive circuit as a function of frequency. The results of such a study of photoconducting silver chloride are given in this paper.

In general, it is necessary to make a detailed analysis in order to interpret the frequency response and so fully understand the photoconducting processes. However, in some cases the photoconductor electrode system can be represented by a combination of linear circuit elements. It is shown that it is useful to describe the photoresponse of the silver chloride electrode system for the conditions of the experiments reported here by such an equivalent circuit. Deviations are discussed in terms of space charge and other nonlinear processes. The data are also briefly compared with the results of an analysis by MacDonald[1] from which some observations can be predicted, although the assumed boundary conditions are not equivalent to those of this investigation.

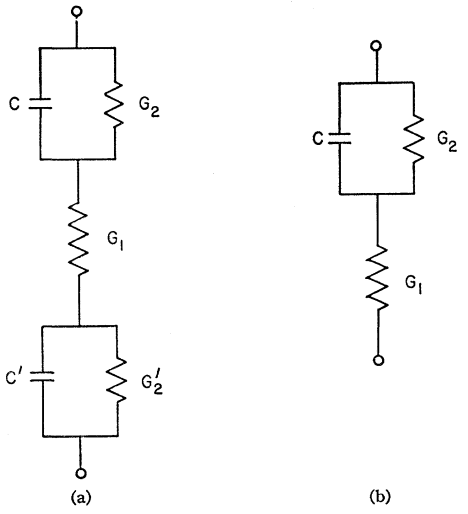


FIG. 1. Equivalent circuits.

The work reported in this paper was undertaken as part of a more general study of the transport, recombination and trapping processes of electrons and holes in an ionic solid.[2,3] In this paper only observations pertaining to the understanding of the photoconductive processes are considered.

## II. EXPERIMENTAL PROCEDURE

Most of the experimental conditions have been reported elsewhere.[2,3] The samples were mounted in a vacuum cryostat and were exposed only to weak red light except at low temperatures. The silver chloride crystals, which are described elsewhere, were grown at Cornell and at the Kodak Research Laboratories.[2,4,5] After working to the desired dimensions by machining or grinding on a ground glass plate with a sodium thiosulfate (30%) solution the samples were etched in ammonium hydroxide or hydrochloric acid and washed in conductivity water. Evaporated gold or painted graphite (water solution) electrodes were then applied. Samples of two geometries have been used. Some were in the form of thin wafers 0.025 cm in thickness and 1.0 cm in diameter and had electrodes applied to the flat surfaces. Irradiation was through one electrode and in the direction of the applied field. Other samples were in the form of bars 0.2×0.2×2.0 cm with electrodes on

* Research supported by the National Science Foundation and the U. S. Atomic Energy Commission.

† The experimental parts of this work were completed at Cornell University, Ithaca, New York.

[1] J. R. MacDonald, Phys. Rev. **92**, 4 (1953).
[2] D. A. Wiegand, Phys. Rev. **113**, 52 (1959).
[3] D. A. Wiegand, thesis, Cornell University, Ithaca, New York, 1956 (unpublished).
[4] N. R. Nail, F. Moser, P. E. Goddard, and F. Urbach, Rev. Sci. Instr. **28**, 275 (1957).
[5] The author is indebted to Dr. F. Urbach of the Kodak Research Laboratory and Mr. G. Slack of Cornell University for making silver chloride crystals available.

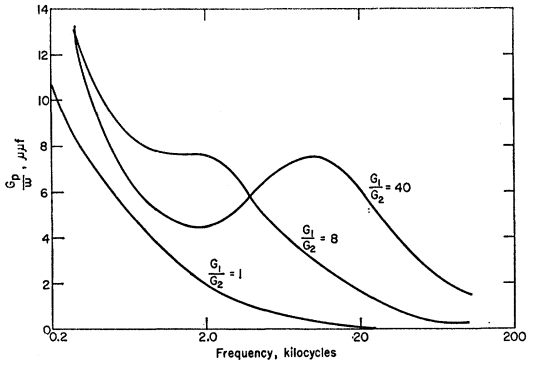


FIG. 2. Calculated frequency response of $G_p/\omega$ of the circuit of Fig. 1(b). $C=15\ \mu\mu f$ and $G_2=2.4\times10^{-8}$ ohm$^{-1}$.

two opposite 0.2×2.0 faces. Irradiation was normal to a third 0.2×2.0 face and thus perpendicular to the applied field. While the nominal wavelengths of exciting light were 3650 and 3840 A as determined from monochromator settings it was generally necessary, for reasons of intensity, to use very large slit widths. The conductance and capacitance of the sample-electrode system were measured by a type 716-C General Radio capacitance bridge. All values reported are differences between the conductance and capacitance with and without illumination. Therefore, lead capacitance and losses have been eliminated. In most cases the losses without excitation were negligible compared to those during excitation.

## III. PHOTORESPONSE

### General Observations

A photoconductor-electrode system might be represented by the circuit of Fig. 1(a), where $G_1$ is the bulk photoconductance, $G_2$ and $C$ represent the conductance and capacitance at one electrode, and the primed quantities the conductance and capacitance at the other electrode. In general, these circuit elements will not be linear and in general it will be necessary to consider a capacitance in parallel with $G_1$. For the special case of ohmic contacts only $G_1$ must be considered, while in the case of blocking electrodes $G_2$ and $G_2'$ become zero. Since it is also possible that one electrode can be partially blocking and the other not, the circuit of Fig. 1(b) is of interest. The frequency responses of the two circuits of Fig. 1 are similar and only case 1(b) is considered in detail. Expressions for the equivalent parallel conductance $G_p$ and capacitance $C_p$ are derived in the Appendix. The frequency response of $G_p/\omega$ represented in Fig. 2, is very sensitive to the ratio $G_1/G_2$. For $G_1/G_2<8$, $G_p/\omega$ decreases monotonically with increasing frequency; for $G_1/G_2>8$ the curve contains a minimum and a maximum, and for $G_1/G_2=8$ a plateau. Since curves of this general type are indeed observed it is interesting to consider this circuit in some detail.

In Fig. 3 observed values of $C_p$ and $G_p/\omega$ are plotted vs frequency. Also shown are the calculated values based on the circuit of Fig. 1(b), where the parameters have been chosen to match the frequencies of the maximum and minimum and to give approximately the same low-frequency capacitance as the measurement. The degree of similarity of the observed and calculated curves indicates in a rough fashion the degree to which the sample-electrode system can be represented by the equivalent circuit of Fig. 1(b). (Other data are presented in Fig. 7.) Deviations are of course to be expected since the nonlinear sample-electrode is being replaced by linear circuit elements. These deviations are discussed below.

Similar frequency responses have been observed in many samples of both the wafer and bar type, made from both the Cornell and the Kodak grown material. Graphite and gold electrodes have been used as well as direct contacts between the sample and copper supports. It therefore seems reasonable to conclude that the observed frequency response is characteristic of silver chloride for the condition of these experiments, and that it is meaningful to discuss the photoresponse in terms of the equivalent circuit parameters. While $G_1$ is to be associated with the bulk photoconductivity of the sample, $G_2$ and $C$ can be due to potential barriers at the electrodes or possibly internal to the sample, such as at grain boundaries. However, $G_2$ could also be associated with regions of different and generally lower conductivity than $G_1$, such as sections where the electron lifetime or mobility are smaller. The lifetime may be decreased because of higher densities of traps or recombination centers, whereas the mobility could be reduced by scattering centers, such as ionized impurities. Both of these effects may then be brought about by high local densities of imperfections such as might be found in surface layers. Since both surfaces near the electrodes will be affected the equivalent circuit (a) rather than (b) should be used. However it is reasonable to assume that both surfaces behave in an identical way, in which case model (b) is essentially equivalent to model (a).

$G_p$ and $C_p$, and thus the parameters $G_1$, $G_2$, and $C$ depend on the intensity and wavelength of the exciting radiation, on the applied voltage and on the tempera-

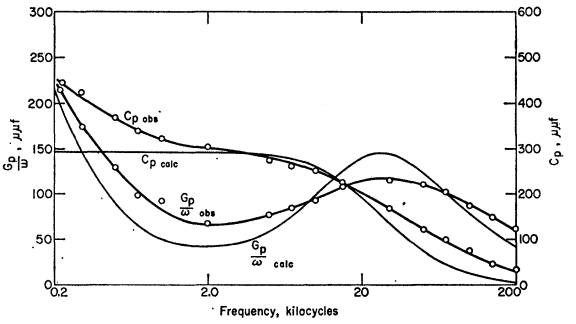


FIG. 3. Comparison of observed and calculated frequency response of $C_p$ and $G_p/\omega$.

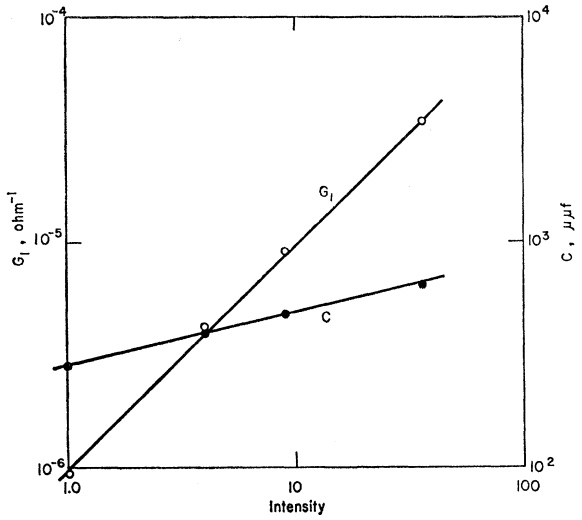


FIG. 4. $G_1$ and $C$ vs relative intensity.

ture. Because of these observations it is possible to put some limitations on possible interpretations. The measurements, preliminary in nature, have in general been made on only a few samples and the data are presented in the following sections. It must, however, be noted that some lack of reproducibility has been observed. After slight mechanical disturbances, or after warming to room temperature and recooling, it was not always possible to obtain the same data points, and changes of the order of 20 to 30% have been found. The general frequency response was, however, unchanged. While no attempt was made to cool samples slowly, the warming rate was determined by the cryostat and several hours were required to warm from liquid nitrogen temperature to room temperature. Since these variations have been observed in both the bar and wafer samples, they cannot be caused by changes in the geometry, but seem related to the properties of the material. It is suggested that these changes in photoresponses are due to inhomogeneities in the samples. Waldner[6] observed much larger inhomogeneities in measuring photocurrent decay times in Cornell grown material.

The following relationships, derived in the Appendix, are needed for a quantitative interpretation of the experiments. The frequencies $f_r$ and $f_m$ for the maximum and minimum in the curve of $G_p/\omega$ vs frequency, for the case of $G_1/G_2 \gg 4$ are given by

$$\omega_r = 2\pi f_r \simeq G_1/C; \quad \omega_m = 2\pi f_m \simeq (G_1G_2)^{\frac{1}{2}}/C, \quad (1a)$$

from which

$$(\omega_r/\omega_m)^2 \simeq G_1/G_2. \quad (1b)$$

At $\omega = \omega_r$,

$$G_p \sim G_1/2; \quad C_p \sim C/2. \quad (2)$$

At low frequencies such that $(G_1/\omega C)^2 \gg 1$

$$C_p \simeq C. \quad (3)$$

[6] M. Waldner, thesis, Cornell University, Ithaca, New York, 1954 (unpublished).

Because of relationships 1, 2, and 3, the parameters $G_1$, $G_2$, and $C$ are easily determined from the curves of $G_p/\omega$ and $C_p$ vs frequency whenever there are pronounced maxima and minima and the appropriate portions of the curve lie within the frequency range of measurement. Alternatively, a curve fitting process outlined in the Appendix may be used.

## Intensity and Wavelength Dependence

Measurements have been made of the dependence of $G_p/\omega$, and $C_p$ on intensity in the frequency region around $f_r$. Relative intensities were determined from sample to light source distance. From Eq. (2) it is then possible to obtain the intensity dependence of $G_1$ and $C$ and these are given in Fig. 4. While $C$ is relatively insensitive to intensity, $G_1$ increases linearly indicating that the bulk photoconductance increases linearly with intensity. The frequencies $f_r$ as calculated from Eq. 1(a) and $G_1$ and $C$, determined from Eq. (2), are within 15% of the observed values for all intensities. Unfortunately, $G_p$ and $C_p$ were not taken over a sufficiently wide frequency range to be able to determine $f_m$, and thus $G_2$. However, by a crude curve-fitting process it is possible to obtain an estimate of $G_2$. These calculations indicate that $G_2$ increases in approximately the same fashion as $G_1$ with intensity.

The photoresponse is a function of wavelength for a variety of different experimental conditions and has a maximum in the vicinity of 3840 A.[3,7–9] The curves of $G_p/\omega$ and $C_p$ also depend on $\lambda$. In a particular case an increase of wavelength from 3650 to 3840 A increased $G_1$ by a factor of 6 and increased $C$ by approximately a factor of 2 as determined by Eq. (2). $f_r$ increased in the manner predicted by Eq. (1). These results are consistent with the intensity dependence of $G_1$ and $C$. An increase in $G_1$, brought about presumably by an increase in the total number of free carriers either by varying the wavelength or the intensity, is associated with a smaller increase in $C$. The wavelength dependence of $G_2$ was not determined. It should be noted that the absorption constant is approximately $2\times10^2$ cm$^{-1}$ at 3650 A and 10 cm$^{-1}$ at 3840 A.[7] However, because of the wide monochromator slit widths used here the difference in the effective absorption coefficients at the two wavelengths is considerably smaller. An explanation of the maximum at 3840 A in terms of bimolecular recombination processes has been advanced by Gilleo,[7] while an explanation in terms of a defective surface layer is given by Van Heyningen and Brown,[8] and Gordon.[9]

[7] W. Caldwell, thesis, Cornell University, Ithaca, New York, 1948 (unpublished); J. Nanda, thesis, Cornell University, Ithaca, New York, 1949 (unpublished); M. Gilleo, Phys. Rev. **91**, 534 (1953).

[8] R. Van Heyningen and F. C. Brown, Phys. Rev. **111**, 462 (1958).

[9] A. Gordon, Phys. Rev. **122**, 748 (1961).

### Voltage Dependence

Although detailed measurements were not taken as a function of voltage it was observed that the curves of $G_p/\omega$ and $C_p$ were sensitive to this parameter. The most notable result is that $C$ decreases with increasing voltage while $G_1$ is insensitive to voltage. $f_r$ varies with voltages as predicted by Eq. (1a) and the values of $G_1$ and $C$ obtained by Eq. (2). The sensitivity of $C$ to voltage is apparently somewhat dependent on the magnitude of the voltage. In one case, an increase of the voltage from 0.1 to 0.60 v decreased $C$ by a factor of only 0.7, and in another an increase of the voltage from 0.5 to 1.0 v decreased the capacitance by 0.8. However, when the voltage was increased from 0.5 to 5.0 v the capacitance decreased by a factor of 0.3.

Wood[10] found that $C_p$ varied as the inverse square root of voltage for values from 0.5 to 100 v at low frequency. However, because the relative values of $G_1$, $G_2$, and $C$ have not been determined in Wood's case, it is not possible to relate directly this voltage dependence of $C_p$ to a voltage dependence of $C$. While it is not possible with the data available to determine the voltage dependence of $G_2$ unambiguously, it is possible to deduce that for changes in voltage of a factor of 2, $G_2$ either increased slightly or remained unchanged.

It is important to note that since these are ac measurements, the voltage applied to $C$ and $G_2$ varies from zero to the maximum value during each cycle. The voltage referred to above is the maximum value. A dependence of $C$ and $G_2$ on voltage makes the circuit nonlinear and thus the values determined from the data are time averages. It is also necessary to consider that because the applied voltage was maintained constant while the frequency was varied the voltage across $C$ decreased with increasing frequency, thus tending to cause an apparent increase of $C$ with frequency. Deviations from the predictions of the circuit of Fig. 1(b) can then be expected because of this dependence of $C$ and $G_2$ on voltage. Further investigations might be best carried out with a dc bias and a much smaller ac signal applied to the sample. However, space-charge effects in the bulk of the sample may then become more important.

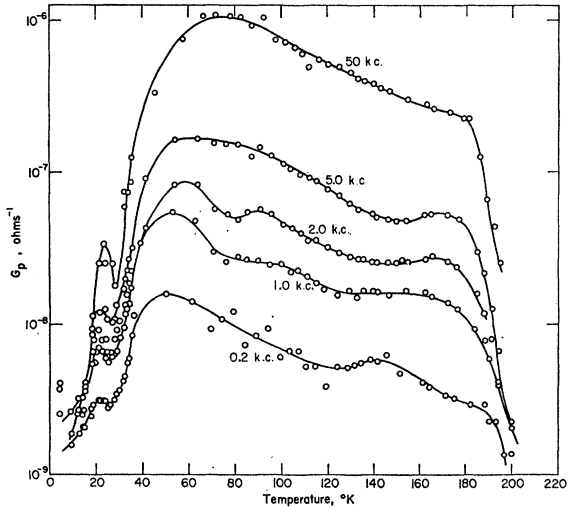


FIG. 5. $G_p$ vs temperature for several frequencies.

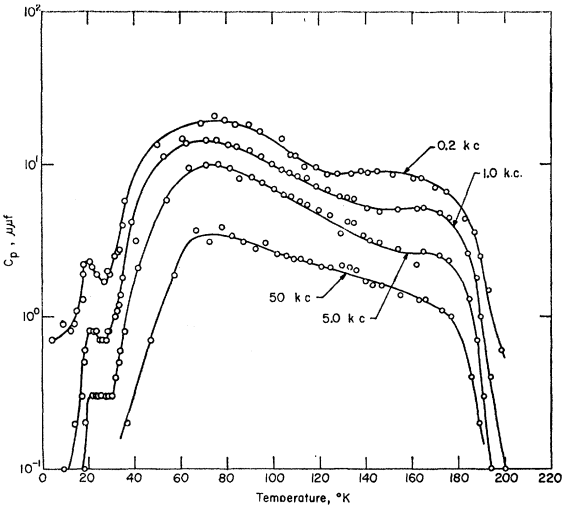


FIG. 6. $C_p$ vs temperature for several frequencies.

### Photoresponse vs Temperature

The general trend of the temperature dependence of the photoresponse is similar to that reported by others.[10,11] In Figs. 5 and 6, $G_p$ and $C_p$ are given as a function of temperature for a few frequencies, and in Fig. 7, $G_p/\omega$ is given vs frequency for a few temperatures. In Fig. 5, data at $f=2.0$ kc/sec are presented over a limited temperature range for the purpose of clarity. The data of Fig. 7 can be compared with the calculated curves of Fig. 2. $C$ and $G_1$ at $G_1/G_2=40$ were chosen to match the experimental data at $T=75°$K while $G_2$ is somewhat larger than the value obtained from Fig. 7, at the same temperature. In comparing the curves of Figs. 2 and 7 it must be remembered that the curves of Fig. 2 were calculated for constant $G_2$ and $C$, but variable $G_1$, while all three of the circuit parameters are actually functions of temperature. In general, the curves are of the type to be expected from the circuit of Fig. 1(b), although there are deviations. Because of these deviations, detailed curve fittings seem unwarranted at this time. It is, however, possible to make a few general statements about the temperature dependence of $G_1$, $G_2$, and $C$.

At frequencies such that $(G_1+G_2)^2/(2\pi C)^2 \ll f^2$, $G_p$ approaches $G_1$. Since this condition is satisfied for 50 kc/sec, the temperature dependence of $G_1$ is given by

[10] R. Wood, thesis, Cornell University, Ithaca, New York, 1953 (unpublished).

[11] W. Lehfeldt, Nachr. Ges. Wiss. Göttingen 1, 171 (1935), Fachgruppen II.

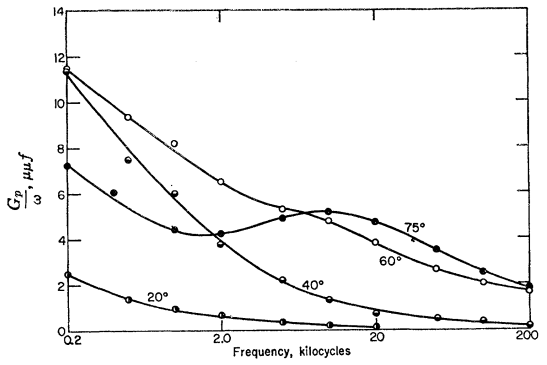


FIG. 7. $G_p/\omega$ vs frequency at several temperatures. Taken from the data of Fig. 5.

the curve of $G_p$ at 50 kc/sec in Fig. 5. At low frequencies, such that $G_2(G_1+G_2)/(2\pi C)^2 \gg f^2$, $G_p$ and $C_p$ are independent of frequency and given by

$$G_p \simeq \frac{G_2}{1+G_2/G_1}; \quad C_p \simeq \frac{C}{(1+G_2/G_1)^2} \tag{4}$$

so that, at these frequencies, $G_p \simeq G_2$ and $C_p \simeq C$ when $G_1/G_2 \gg 1$. However, the results of curve fitting indicate that $G_1/G_2$ increases from approximately 1 at 10°K to 30 at 75°K, therefore indicating that the temperature dependence of $G_p$ and $C_p$ at low frequencies (Figs. 5 and 6) reflects not only the temperature dependence of $G_2$ and $C$, but also that of $G_1/G_2$. The changes of $G_p$ and $C_p$ at 0.20 kc/sec of Figs. 5 and 6 then give upper bounds to the changes of $G_2$ and $C$. While the curve fitting data indicates that $G_1$ increases by more than two orders of magnitude between 10° and 75°K, $C$ increases by approximately an order of magnitude. It is to be noted that as a function of intensity and wavelength, $G_1$ also changed by a much larger percentage than $C$. The curve-fitting results can be taken only as suggestive because this process is only approximate, and the values of the three circuit parameters are such that at the lowest and highest temperatures the geometrical capacitance of the sample should be included in the equivalent circuit.

The increase of the ratio $G_1/G_2$ as temperature is increased from 10° to 75°K is then evidenced by the appearance of a plateau in the curve of $G_p/\omega$ vs frequency at $T=65$°K and a pronounced maximum at 75°K (Fig. 7). The prominence of the maximum decreases with increasing temperature above 75°K because of a decrease in $G_1/G_2$ and a plateau is observed in the vicinity of 120°K.

The maxima in Fig. 5 shift to higher temperatures with increasing frequency, while those in Fig. 6 are not frequency dependent. In addition, the maxima of Fig. 6 occur at the same temperature as in the high-frequency curve of Fig. 5. All of these observations can be explained in terms of the dominance of the temperature dependence of $G_1$. It is shown in the Appendix that for constant $G_2$ and $C$ and $\omega > G_2/C$, $G_p$ passes through a maximum as $G_1$ increases, while $C_p$ is a monotonic function of $G_1$. In addition, the maximum of $G_p$ shifts to higher values of $G_1$ as the frequency is increased, for frequencies above approximately 0.5 kc/sec, and is outside the $G_1$ range in these experiments for $f>10$ kc/sec. The temperature dependence of $G_p$ and $C_p$ in the vicinity of 75°K can then be explained in terms of these relations.

If $G_1$ alone were responsible for the observed temperature dependence of $G_p$, then a second maximum of equal magnitude should be observed when $G_1$ decreases above 75°K. An indication of this is observed at 2.0 kc/sec at $T=90$°K (Fig. 5). That this second maximum is not observed at all frequencies suggests that $G_2$ is changing more rapidly above 75°K than below it. A very shallow minimum between the two maxima would not be observable because of the scatter of data points.

An important result of the temperature dependence of $G_p/\omega$ is that $f_r$ decreases with increasing temperatures between 75° and 120°K, thus indicating that a time constant which might be associated with $f_r$ increases with increasing temperature. Therefore it seems that such a time constant cannot be associated with the trapping time of electrons. However, the temperature dependence of $f_r$ is consistent with the temperature dependence of $G_1$ and $C$ as determined by Eq. (2). The calculated and observed magnitudes of $f_r$ are also in agreement.

It is not possible with the data available to describe all of the structure of the curves of Figs. 5 and 6. The maxima in the vicinity of 23°K, which are discussed briefly later, were observed only during this series of measurements. Previous measurements of the total photocurrent in the same sample did not reveal these maxima although a break in the curve was observed at about the same temperature. Data taken by Wood[10] also exhibited a break in the curve at about $T=20$°K. The sample which showed these peaks received ultraviolet irradiation between 80° and 210°K and had passed through many cycles of cooling from room to liquid nitrogen temperature, uv irradiation, and then warming to room temperature between the two sets of measurements. Observation on a fresh sample taken from the same piece of AgCl did not show this structure. The data of Figs. 5 and 6 have not been corrected for the temperature dependence of the absorption coefficient of AgCl and thus for changes in the density or distribution of the absorbed photons.

## IV. DISCUSSION

### Observations at 80°K

The data indicate that an explanation of the photoresponse in terms of the equivalent circuit parameters must satisfy the following: (1) $G_2$ and $C$ are approximately linear circuit elements; (2) $C$ does, however, decrease with increasing voltage; (3) $G_2$ increases with

light intensity; (4) $C$ changes in the same fashion but to a lesser degree than $G_1$, as a function of intensity, wavelength, and temperature. In addition, the variations of $G_1$, the bulk photoconductance, with the various quantities must be considered. A discussion of $G_2$ and $C$ is followed by a brief discussion of $G_1$.

The dependence of $C$ on voltage suggests that this capacitance is associated with an exhaustion region and it is interesting to consider the possibility that this exhaustion region is due to a potential barrier at the sample electrode interface. For the conditions of this experiment there will be then a forward biased junction at one electrode and a reversed biased junction at the other. The impedance of the forward biased junction should be negligible compared to the reversed biased junction and the bulk of the sample. If this were not true the equivalent circuit would be that of Fig. 1(a) rather than Fig. 1(b) with the primed and the unprimed quantities not equal. The exhaustion region occurs at the reversed biased junction. Potential barriers could also occur at internal boundaries.

For the exhaustion layer the dependence of the capacitance on voltage is related to the distribution of positive charge in the layer and to the height of the barrier. For a Schottky type layer the differential capacitance is given by

$$C=\left(\frac{e\epsilon_0 K_s N}{2(V_B+V_D)}\right)^{\frac{1}{2}} A=\frac{\epsilon_0 K_s}{l_s}A, \qquad (5)$$

where $V_B$ is the portion of the applied voltage across the junction, $V_D$ is the potential height as seen from the AgCl, $N$ is the density of positive charge, $K_s$ is the dielectric constant, $\epsilon_0$ is the permittivity of free space, $l_s$ is the thickness of the barrier region, and $A$ is the area.[12] By taking $(V_B+V_D)$ of the order of a volt, $A=0.2$ cm$^2$, $K_s=12.3$, and $C=300$ $\mu\mu$f for the conditions of Fig. 3, we find $N\simeq 5\times 10^{13}$ cc$^{-1}$ and $l_s\simeq 5\times 10^{-4}$ cm. Since in some cases $C$ is an order of magnitude smaller, the barrier thickness can be proportionally larger. The positive charge in the exhaustion region may be associated with ionized donors, trapped holes, or valence band holes if the mobility is sufficiently small.[13,14] While it is assumed in obtaining Eq. (5) that $N$ is constant as a function of distance from the barrier, the actual spacial distribution of $N$ can be determined by detailed measurements of $C$ vs voltage. The capacitance $C$ from Eq. (5) may increase with light intensity or wavelength either because of an increase of $N$ or a decrease of $V_D$. Since $C$ varies monotonically with $G_1$ and so presumably with the density of mobile electrons, it seems reasonable to conclude that $N$ is determined, at least in part, by holes produced by illumination and that the changes in $C$ are due primarily to changes in $N$.

It is interesting to consider briefly the current through this type of barrier. If the barrier current is determined by a reverse-biased junction it is important to note that it is related only to electron emission into the silver chloride and to diffusion in the barrier region. Thermionic emission is considered in the diode model but in addition diffusion is considered in the diffusion model.[12] While neither the diode nor the diffusion models predict linear current-voltage characteristics, Henish[12] has shown that when image forces and tunneling are considered the current-voltage curve can, in some cases, be approximately linear. It therefore may be reasonable as a first approximation to represent the barrier current by the circuit parameter $G_2$. It is not clear, however, in the present case whether the diffusion model or the diode model is appropriate. Estimates of the mean free path (see Mott and Gurney[15] and Low and Pines[16]) give values of the order of $10^{-6}$ cm at 80°K and thus much smaller than the barrier thickness, suggesting considerable scattering in the barrier region. While it is therefore difficult to specify the detailed processes, it is at least possible that the current-voltage characteristic is determined in this case by a combination of electron scattering in the barrier layer region and the effective dependence of the potential barrier height on image forces and tunneling.

An increase in barrier current, and thus in $G_2$, with increasing light intensity can be attributed to image force effects or tunneling. The increase in $C$ with intensity (Fig. 4) indicates that $N$, the density of positive charge in the barrier region, has increased. This increase in $N$ will increase the field at the metal-electrode interface and so decrease the barrier height in the same manner that the work function of a metal is decreased by an external field when the image force is considered.

In the above discussion it is assumed that hole currents are negligible but that holes are produced throughout the volume of the photoconductor. However there are observations which indicate that it may be necessary to consider hole motion. The bar samples have been illuminated such that either the whole region between electrodes was excited or such that only a slab parallel to the electrodes but isolated from both was in the light beam. The wafer samples have always been irradiated through one electrode such that electrons and holes should be produced throughout the region between the electrodes. Therefore if holes are completely immobile, quite different space charge conditions should be found for these different conditions of excitation. However, the same general frequency response is observed for the various conditions and the values of $G_2$ and $C$ are approximately the same. This will be the case only if electrons and holes can diffuse throughout

[12] H. K. Henish, *Rectifying Semiconductor Contacts* (Oxford University Press, New York, 1957), pp. 202, 214.
[13] F. C. Brown, Phys. Rev. **97**, 355 (1955); M. Werman, thesis, Cornell University, Ithaca, New York, 1956 (unpublished); M. Werman, Office of Naval Research Technical Report No. 1, NR 014-402, 1956 (unpublished).
[14] A. Michel, Phys. Rev. **121**, 968 (1961).
[15] N. F. Mott and R. W. Gurney, *Electronic Processes in Ionic Crystals* (Oxford University Press, New York, 1948), p. 104.
[16] F. Low and D. Pines, Phys. Rev. **98**, 414 (1955).

the volume of the crystal in those cases of nonuniform illumination. In addition the capacitance increases monotonically with the bulk conductivity as a function of intensity, wavelength, and temperature. This can be attributed to an increase in the density of holes in the exhaustion region only if the holes are produced in the exhaustion region or can diffuse to this part of the crystal. The similarity of the data when all or only a portion of the sample is illuminated suggests that the exhaustion region is near the surface. Alternatively it may be possible to produce electrons and holes outside of the region of illumination by radiative transfer of energy resulting from electron and hole recombination or exciton decay in the region of illumination.

If holes are mobile it is necessary to consider this possible contribution to a barrier current since there should not be a potential barrier to hole motion if there is a barrier to electron motion. An approximately linear current-voltage relationship and a $G_2$ proportional to $G_1$ as a function of intensity may then be reasonable. The dependence of $C$ on voltage and intensity will depend on the ratio of mobile to trapped holes. If the density of mobile holes is approximately the same as the density of mobile electrons in the bulk of the insulator, the data indicate that the density of trapped holes should be much greater than the density of mobile holes. In this case the explanation of the dependence of $C$ on voltage and intensity is unaltered.

The above discussion is given in terms of an exhaustion layer associated with a potential barrier at the sample electrode interface, where the height of the barrier is determined either by the appropriate work function and electron affinity or by surface trapping. The insensitivity of the results to the type of electrode suggests that the barrier height is determined by trapping.[12,17] Surface trapping in this context is considered to take place in a layer of a few angstroms thickness rather than in the thick layers of the exhaustion region. The negative charge could however be distributed throughout a layer of the thick type at the surface due to a local high density of traps as proposed by Van Heyningen and Brown[8] and others.[9,14,17a] The above discussion is not altered in a qualitative way for a barrier of this sort as there still will be an exhaustion region between the thick surface layer of electron traps and the bulk of the sample. If the trapping in a thick surface layer is important the frequency response should be a function of surface preparation.

It is also possible to associate $G_2$ with a region at the surface having a lower conductivity than the bulk due to lifetime or mobility considerations. If trapping and possible space charge in this region are neglected, the equivalent circuit will be that of Fig. 1(a) where $G_2 \simeq G_2'$. If holes are immobile there will be, when a voltage is applied, an exhaustion region between the bulk and the surface layer at the negative electrode. This case is attractive because of the possibility of obtaining a linear barrier conductance which increases with intensity in the same fashion as $G_1$. Of course it may be necessary to consider a low-conductivity region near the surface in addition to a potential barrier at the sample electrode interface.

It is necessary to discuss briefly a third and completely different interpretation of the frequency response of the AgCl-electrode system. In all cases at 80°K in which a maximum in the curves of $G_p/\omega$ vs $f$ has been observed, the photocurrent decay time has been of the order of milliseconds or larger, while when the maximum was not observed the decay time was generally of the order of microseconds.[2,3] In particular, the decay time of silver chloride as grown at Cornell has been in many cases short and a maximum in the curve of $G_p/\omega$ vs $f$ was not observed. However, after annealing in vacuum at 400°C for eight hours and slow cooling the decay time was increased appreciably and a maximum appeared. In one case an annealed wafer-type sample contained regions of slow decay and at least one region of fast decay. The regions of slow decay showed a maximum while the other did not. The photocurrent decay of as-grown silver chloride obtained from Kodak was of the slow type at 80°K and a maximum was observed. Since on the basis of the circuit of Fig. 1(b) a maximum is observed only if $G_1/G_2 > 8$, annealing must increase this ratio. If it is assumed that the photocurrent decay time is a measure of the electron lifetime, a slow decay indicates a long lifetime and thus a large value of $G_1$. Therefore the relationship can be explained qualitatively in terms of this circuit.

It is also possible, however, to explain this relationship between the decay time and the frequency response by another model, a kinetic analysis of which has been given by MacDonald.[1] He has found a relaxation process, observable as a maximum in the curve of $G_p/\omega$ vs $f$, associated with the transit time of the carriers which is analogous to that found for the circuit of Fig. 1(b). However, in addition he has found a relaxation associated with the lifetime of the carriers which is observed only when the lifetime is above a minimum value. The latter result is similar to the behavior observed here. MacDonald has made several assumptions, including the following: blocking electrodes, bimolecular recombination, and no trapping. A lifetime-dependent relaxation is then found whenever the lifetime is sufficiently greater than the transit time through the sample. This model predicts the correct direction for the changes of $f_r$ for most of the observations. However, the above assumptions make it difficult to apply this model to silver chloride under the experimental conditions used in this investigation. The frequency responses clearly indicate that the electrodes are not completely blocking, the photocurrent characteristics have never been observed to be strongly

[17] J. Bardeen, Phys. Rev. **71**, 717 (1947).
[17a] Evidence for trapping in the surface layers is also given by A. M. Goodman and G. Warfield, Phys. Rev. **120**, 1142 (1960).

bimolecular, and trapping is certainly important.[2] In addition, a second relaxation process, predicted by MacDonald's analysis, has never been observed. On the other hand, the relaxation frequency $f_r$ behaves as predicted by the circuit of Fig. 1(b) on the basis of the observed dependence of $G_1$ and $C$ on intensity, voltage, wavelength, and temperature. In addition, there is evidence that the photocurrent decay is dependent on trapping characteristics and not directly on the electron lifetime.[2,3] It therefore seems reasonable to conclude at this time that the structure of the curve of $G_p/\omega$ vs $f$ is not directly associated with the electron lifetime as predicted by the model analyzed by MacDonald. The electron lifetime and trapping may be altered by annealing so that an increase in the photocurrent decay times could indicate a change in both, while an increase in $G_1$ indicates an increase in lifetime. In addition, surface states, and thus the potential barrier, may be altered by annealing. For these reasons it is not surprising that the ratio $G_1/G_2$ can be increased by the annealing procedure.

$G_1$ is assumed to be the bulk conductivity of the sample and therefore is the quantity generally of interest in photoconduction experiments. In the absence of space charge outside of the barrier region we have

$$G_1 = N_e e \mu A/l, \tag{6}$$

where $N_e$ is the steady-state density of conduction electrons, $\mu$ the microscopic mobility, and $A$ and $l$ are the appropriate dimensions. Since the circuit is approximately linear we might suspect that space charge is not important outside of the exhaustion region. This is reasonable if the forward biased barrier does not offer high impedance to charge motion. An estimate of the possible importance of space charge can be made by comparing the carrier transit time to the period of the applied field. Of course space charge effects will be most important at low frequencies. The rise of the observed $C_p$ above the calculated value as shown in Fig. 3 at low frequencies might be due to such effects. However, since similar frequency responses have been found for both the bar and wafer samples in which the transit times are quite different, it is suggested that space charge is not important and that the forward biased barrier does not impede charge motion. If $G_2$ is associated with a region of low conductivity rather than a potential barrier, space charge may be important if electrons become trapped in this region and the holes are not sufficiently mobile to neutralize the electron charge.

From the data of Fig. 4, if space charge is assumed negligible, the average density of electrons in the conduction band is found from Eq. (6) to increase from $10^{10}$ to $3\times10^{11}$ per cc as the intensity is increased. The mobility is obtained from the work of Brown.[13] A linear increase of $N_e$ with intensity deduced from the data of Fig. 4 indicates that the recombination processes are monomolecular.

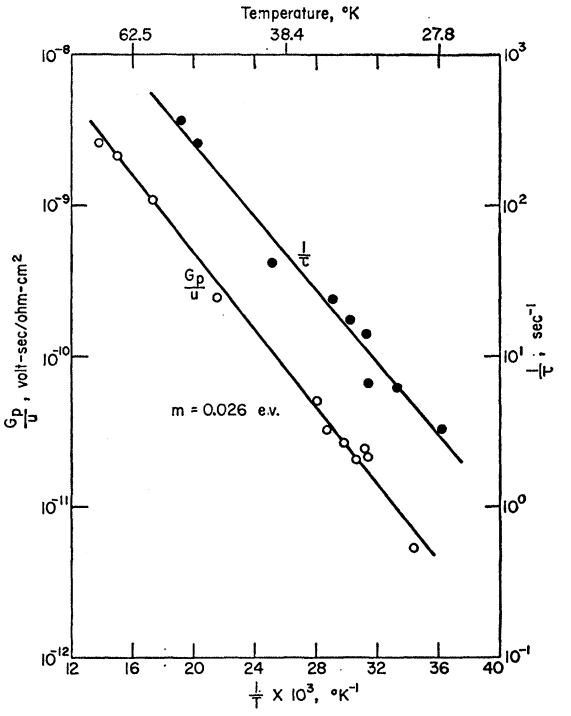


FIG. 8. $G_p/\mu$ and $1/\tau$ vs $1/T$. $G_p$ is taken at 50 kc/sec. $\tau$ is the time constant of an exponential portion of the photocurrent decay curve (see text).

## Temperature Dependence

It is instructive to consider briefly the temperature dependence of the three circuit parameters. A discussion of $G_1$ is followed by a few remarks about $C$ and $G_2$. In the absence of space charge the bulk photoconductance, $G_1$ is given by Eq. (6) where only $N_e$ and $\mu$ are functions of temperature. The mobility as determined from Hall measurements[18] decreases monotonically with increasing temperature. Between 75° and 180°K, $G_1$ decreases slightly faster than $\mu$, indicating only a small decrease in $N_e$, perhaps by a factor of 2. Below 75°, $G_1$ increases rapidly with temperature; thus $N_e$ must also increase. This can come about by a decrease of the time electrons spend in traps. It could also be caused by a decrease in efficiency of recombination, or by thermal excitation of electrons from excited states in the forbidden band into the conduction band. However, according to Van Heyningen and Brown[8] the quantum yield of photoexcitation does not increase appreciably between 6.5 and 80°K. In addition the luminescence is temperature independent in this temperature range, but appears to be associated with the same trapping levels as the photoconductivity.[2,3]

In comparing the present results with the mobility measurements mentioned above, one has to bear in mind that the Hall measurements were made by a pulse method with very low total light intensity, while the

[18] K. Kobayashi and F. C. Brown, Phys. Rev. **113**, 507 (1959).

measurements here were made under steady illumination. It is known that the photoresponses under these two conditions are very different and it is possible that the values of the mobility will be different and that the temperature coefficient may even change its sign. Also differences in the purity and perfection of the crystal may give rise to differences in the temperature dependence of the mobility.

In the following, trapping will be assumed as an important factor in the temperature dependence of $G_1$. A comparison with the photocurrent decay after removal of illumination, where trapping is also important, is indicated. This decay shows an exponential tail between 28° and 52°, whose time constant $\tau$ decreases exponentially with increasing temperature. A plot of $\ln(1/\tau)$ vs $1/T$ yields a straight line (see Fig. 8) whose slope corresponds to an activation energy of 0.026 ev. If we assume that the measured decay is a measure of the decay of $G_1$ (see next section), then this data suggests a trapping level with this thermal activation energy. $G_1$, as determined from $G_p$ at high frequencies also increases exponentially with increasing temperature between 30° and 65°K with an activation energy of about 0.01 ev. If a quantity proportional to $N_e$ is calculated by dividing $G_1$ by the Hall mobility referred to above, an activation energy of 0.027 results, about equal to that of the decay time, as shown in Fig. 8. This suggests strongly that the temperature dependence of $\tau$ and $N_e$ are related to the same trapping process. Data of the type of Fig. 8 are unfortunately available for only one sample. However, the general behavior of $G_1$ and $\tau$ in other samples is very similar.

The meaning of the slopes obtained from Fig. 8 is, however, dependent on the kinetics of trapping and recombination. As an example, consider that the total density of excited electrons is $N'$ but that the fraction of time in the conduction band is determined by the trapping time $\tau_T$ and the time for escape from traps $\tau_e$. The density of electrons in the conduction band is then

$$N_e=[N'\tau_T/(\tau_T+\tau_e)]\simeq N'\tau_T/\tau_e=N'\tau_T b_0 e^{-E/kT}, \quad (7)$$

where the approximation is valid when $\tau_e \gg \tau_T$; $\tau_e$ is assumed to vary exponentially with temperature. Since $\tau_T$ will be fairly insensitive to temperature, $N_e$ will increase exponentially with temperature if the kinetics are such as to give a constant $N'$. A similar argument is used by Brown and Kobayashi[19] to explain the temperature dependence of the drift mobility between 40° and 80°K and they deduce an energy of 0.03 ev. Since the time constant of the tail of the conductivity decay can be interpreted as the escape time from traps, the slopes in Fig. 8 give the activation energy for this trap.[2] Alternatively it can be shown that in special cases of second order kinetics the slope of Fig. 8 will be equal to one half of the thermal activation energy associated with the trapping states.[3] It may be mentioned that a slope of 0.05 ev, or approximately twice that of Fig. 8, was obtained from the temperature dependence of the luminescence.[2] However, it seems that a much more detailed study of the kinetics must be made before a valid comparison between luminescence and photoconductivity can be made in this way.

It is possible to associate the maxima of Fig. 5 at about 23°K with the same trapping level discussed above. An extrapolation to 23°K indicates a lifetime of the trapping states of 17 sec. It is therefore possible that this maximum is due to a thermal glow type response superimposed on the steady-state conductivity vs temperature curve. The heating rate in this temperature range was 0.4 degree per minute. The energy associated with a thermal glow process can be estimated from the relationship

$$E=kT_m \ln b_0, \quad (8)$$

where $T_m$ is the temperature of the maximum and $b_0$ is the attempt frequency.[20] From this relationship we find $E=0.054$ ev for $T_m=23$°K and $b_0=10^{12}$ sec$^{-1}$. However, from the $1/\tau$ curve of Fig. 8 an attempt frequency of approximately $10^5$ sec$^{-1}$ is obtained. While this is an exceptionally low value, substitution into Eq. (8) yields an energy of 0.03 ev in satisfactory agreement with the slope of Fig. 8. Nevertheless because of the approximate nature of Eq. (8) the difference between 0.023 and 0.054 may not be significant. More precise methods of obtaining $E$ have been developed for cases where the shape of the glow-curve and a kinetics are known.[21] Van Heyningen and Brown[8] have reported electrical glow peaks in this same temperature range.

The temperature dependence of the capacitance $C$, as deduced from $C_p$ at $f=0.2$ kc/sec, Fig. 6 and from curve fitting, follows the temperature variations of $G_1$, as deduced from $G_p$ at $f=50$ kc/sec, Fig. 5. The fractional change in $C$ is much less than that of $G_1$, as is also the case in the variation with intensity and wavelength discussed earlier. $N_e$, the density of electrons in the conduction band, is found to have the same general temperature dependence as $G_1$ when the mobility is considered [Eq. (6)]. These data then further indicate the possibility that $N$, the net density of positive charge in the exhaustion region [see Eq. (5)], is a monotonic function of $N_e$, thus suggesting further that at least a portion of $N$ arises from holes produced by the illumination. Of course, $V_D$ in Eq. (5), the barrier height, may also be a function of temperature, especially if $V_D$ is determined by surface trapping, since the density of stable traps can be very sensitive to temperature. However, variations of $V_D$ are expected to have a much larger effect on the barrier current, i.e., on $G_2$, than on $C$.

If $G_2$ is associated with a potential barrier, it can be expected to increase exponentially with temperature. However, as noted above, the activation energy associ-

[19] F. C. Brown and K. Kobayashi, J. Phys. Chem. Solids 8, 300 (1958).

[20] J. T. Randall and M. H. F. Wilkins, Proc. Roy. Soc. (London) A184, 366 (1945).

[21] See, for example, A. Halperin and A. A. Braner, Phys. Rev. 117, 408 (1960).

ated with the barrier may itself be temperature dependent. If the height of the barrier is determined primarily by surface trapping as suggested by the insensitivity of the results to the type of electrode, large changes in the barrier height as a function of temperature might be expected. In addition, the temperature variation of $N$ will affect the height of the barrier due to image force or tunneling considerations. It is therefore not unreasonable that $G_2$, i.e., the barrier current, should increase between 10° and 78°K but less rapidly than $G_1$, as observed. While it is not possible from the data available to determine whether $G_2$ increases or decreases between 75° and 120°K, there is certainly no large change in this parameter. Above 120°K a meaningful measure of $G_2$ could not be obtained. If $G_2$ were associated with a region of lower conductivity rather than a potential barrier the increase of $G_2$ between 10° and 75°K would indicate that the density of carriers in this region is not determined by the same kinetics and/or trapping levels as in the bulk.

## V. PHOTOCURRENT MEASUREMENTS

It is apparent from the frequency response of the equivalent circuit that the dependence of the total photocurrent on temperature, intensity, wavelength, and voltage does not give directly the dependence of the bulk photoconductance $G_1$ on these same variables. Instead it is necessary to consider that $G_2$ and $C$ are also functions of the same variables so that, in general, all three circuit parameters must be considered simultaneously. Most often, however, photocurrent experiments are performed to obtain $G_1$ and thus quantities such as the density of carriers or the mobility. In this case, it is sufficient to make the measurements at high frequencies where the barrier is effectively shorted by the capacitance $C$. However, there arises a difficulty because of the stray capacitance in parallel with the sample. The photocurrent is then the difference between the total currents during and without excitation. In the present experiments this difference was small in most cases at high frequencies and thus difficult to obtain accurately. In some experiments a bridge circuit could be used to circumvent this difficulty. If $G_1/G_2 \gg 4$ it is of course possible to obtain all three parameters from Eqs. (1) and (2) if the frequency range is appropriate. Alternately a curve-fitting procedure can be used.

Because deductions about electron trapping have been made from the decay of the photocurrent it is necessary to consider briefly the degree to which this decay follows that of $G_1$. While a detailed study was not made, observations on one crystal indicate that the time of decay to $1/e$ of the initial value is insensitive to frequency between 0.2 and 200 kc/sec, though some minor changes with frequency in the shape of the decay curve were observed. This insensitivity of the decay to frequency can be at least partially understood in terms of the observed intensity dependence of $G_1$, $G_2$, and $C$ at 80°K. $G_2$ is found to increase approximately in the same fashion as $G_1$ with increasing intensity, while $C$ is fairly insensitive to this variable. Since the same conditions can prevail during the decay, it is not unrealistic to assume as a first approximation that $G_2$ is proportional to $G_1$ and that $C$ is constant. The decay time at very high and low frequencies should then be the same as observed, while the initial current decay at intermediate frequencies should differ because in this approximation $C$ does not decay. The actual conditions must be such that the change in the decay time at intermediate frequencies is small. It is also important to note that, within the above approximation the current will be proportional to $G_1$ at all frequencies after $G_1$ has decreased sufficiently so that $G_1 \ll \omega C$. It then seems possible to conclude that the tails of the photocurrent decay curve represent the decay of $G_1$ and of the density of carriers.

## VI. SUMMARY

It has been demonstrated that the silver chloride electrode system can be described by the circuit of Fig. 1(b). The dependence of the capacitance $C$ on voltage indicates an exhaustion layer and possibly a potential barrier, presumably at the sample-electrode interface. From the magnitude of the capacitance, it is deduced that the exhaustion region is thick and the variation of $C$ with intensity, wavelength, and temperature suggests that at least a component of the positive charge in the exhaustion region is due to holes generated by the illumination. An insensitivity of the results to the type of metal electrode or the type of contact, plus the temperature dependence of the barrier current, indicates that the barriers may be determined primarily by surface trapping. Further studies of the barrier can then yield information about the surfaces or surface layers of ionic crystals. The observations can also be described in terms of surface regions of lower conductivity than the bulk. Detailed measurements as a function of intensity and voltage should permit a choice between these two explanations of the data. The observations clearly indicate the necessity of considering the effects of potential barriers and surface layers in the interpretation of photoconduction experiments. The temperature dependence of the bulk conductivity and the photocurrent decay between 10° and 75°K indicate the importance of electron trapping in this temperature range.

## ACKNOWLEDGMENTS

The author is deeply indebted to Professor Henri S. Sack for advice and encouragement throughout the course of this work, and for assistance in preparing the manuscript. He is also indebted to Professor J. M. Radcliffe and Professor S. Mascarenhas for critical readings of an earlier version of this manuscript, to Dr. R. E. Howard and Dr. B. S. H. Royce in addition to the above for many helpful and stimulating discus-

sions, and to A. Ballonoff for reading the final manuscript.

## VII. APPENDIX

The equivalent parallel conductance and capacitance of the circuit of Fig. 1(b) are:

$$G_p=\frac{G_1[1+(G_2/\omega C)^2(1+G_1/G_2)]}{1+(G_2/\omega C)^2(1+G_1/G_2)^2}, \tag{1a}$$

$$C_p=\frac{G_1^2/\omega^2 C}{1+(G_2/\omega C)^2(1+G_1/G_2)^2}. \tag{1b}$$

At low frequencies such that $G_2(G_1+G_2)/(\omega C)^2\gg 1$,

$$G_p\simeq\frac{G_2}{1+G_2/G_1};\quad C_p\simeq\frac{C}{(1+G_2/G_1)^2}. \tag{2}$$

And at high frequencies such that $[(G_1+G_2)/\omega C]^2\ll 1$

$$G_p\simeq G_1;\quad C_p\simeq G_1^2/\omega^2 C. \tag{3}$$

### $G_p/\omega$ vs Frequency

By equating $d(G_p/\omega)/d\omega$ to zero the following relationship is obtained:

$$\omega^4+\omega^2\left(\frac{G_2}{C}\right)^2\left(1+\frac{G_1}{G_2}\right)\left(2-\frac{G_1}{G_2}\right)+\left(\frac{G_2}{C}\right)^4\left(1+\frac{G_1}{G_2}\right)^3=0. \tag{4}$$

Real and positive roots are obtained when:

$$\frac{(2-G_1/G_2)^2}{4(1+G_1/G_2)}\geqslant 1, \tag{5}$$

which is satisfied if $G_1/G_2\geqslant 8$. If $G_1/G_2\gg 4$, the solutions of Eq. (4) are:

$$\omega_m\simeq(G_1G_2)^{\frac{1}{2}}/C;\quad \omega_r\simeq(G_1/C). \tag{6}$$

By substitution of (6) in (1), we obtain:

$$\text{for } \omega=\omega_m:\quad G_p\simeq 2G_2;\quad C_p=C, \tag{7}$$

$$\text{for } \omega=\omega_r:\quad G_p=G_1/2;\quad C_p=C/2. \tag{8}$$

### $G_p$ vs $G_1$

By setting $dG_p/dG_1=0$ the following relationship is obtained:

$$G_1^2[G_2^2-(\omega C)^2]+G_1(2G_2)[G_2^2+(\omega C)^2]+[G_2^2+(\omega C)^2]^2=0. \tag{9}$$

The possible positive root of this equation is

$$G_{1+}=[G_2^2+(\omega C)^2]/[\omega C-G_2], \tag{10}$$

so that $G_p$ contains a maximum, minimum, or inflection point only when $\omega C>G_2$. It can be shown that it is a maximum. For frequencies just above $\omega=G_2/C$, $G_{1+}$ decreases with increasing frequency. However, by differentiation of (10) it is found that $G_{1+}$ increases with increasing frequencies when $\omega>2.41G_2/C$.

### Curve Fitting

The equivalent series conductance and capacitance of the circuit of Fig. 1(b) are

$$G_s=\frac{G_1[1+(G_2/\omega C)^2]}{1+(G_2/\omega C)^2[1+G_1/G_2]}, \tag{11a}$$

$$C_s=C(1+G_2/\omega C)^2. \tag{11b}$$

We then find that

$$G_2=\omega C(C_s/C-1)^{\frac{1}{2}}, \tag{12a}$$

$$G_1=\frac{G_s}{1-(G_s/\omega C_s)(C_s/C-1)^{\frac{1}{2}}}. \tag{12b}$$

It is then possible to obtain $G_1$ and $G_2$ by choosing $C$ to obtain the best fit to Eqs. (12).